Journal of Catalysis **205,** 157–167 (2002)
doi:10.1006/jcat.2001.3437, available online at http://www.idealibrary.com on IDEAL®

Structure Sensitivity of NO Reduction over Iridium Catalysts in HC–SCR

C. Wögerbauer, M. Maciejewski, and A. Baiker[1]

Laboratory of Technical Chemistry, Swiss Federal Institute of Technology, ETH–Hönggerberg, CH-8093 Zürich, Switzerland

Received June 25, 2001; revised October 3, 2001; accepted October 4, 2001

Ir black with different crystallite sizes and Ir–H–ZSM-5 prepared using two different precursors were investigated for their behavior in selective catalytic reduction using hydrocarbons as reducing agents (HC–SCR). Emphasis was given to the study of the influence of time onstream on N_2 yield, the change in Ir crystallite size, and the change in the ratio of Ir : IrO_2. Under reaction conditions at 450°C Ir–H–ZSM-5 did not reach steady-state catalytic behavior within 32 h. In contrast, unsupported Ir black showed higher initial yields of nitrogen and approached steady-state considerably faster. Ir black with the largest crystallite size (45 nm) required the shortest time for reaching steady-state behavior. The influence of crystallite size on the reaction of Ir with O_2 and NO was addressed and related to the increase in N_2 yields with increasing Ir crystallite size in the reduction of NO using propene as a reducing agent. Comparative pulse thermoanalysis studies of NO and O_2 adsorption on Ir black with different crystallite sizes (5–45 nm) revealed that the relative uptake of NO (m_{NO}/m_{O2}) increases strongly with increasing crystallite size. This behavior is due to a strong structure sensitivity of NO adsorption, whereas O_2 adsorption is relatively insensitive to crystallite size. The improved yield of N_2 with increasing crystallite size under HC–SCR conditions is traced to the higher surface concentration of NO relative to O_2 with increasing crystallite size.

Key Words: **unsupported iridium; iridium black; IrO_2; platinum group metals; reduction of NO; HC–SCR; lean DeNO$_x$; NO$_x$ reduction; dispersion; crystallite size; pulse thermal analysis.**

1. INTRODUCTION

NO_x (the sum of NO and NO_2) belongs to the so-called group of classical air pollutants and it is also termed by the World Health Organization (WHO) a key air pollutant (1). Its negative effects on the environment range from the contribution to eutrophication of aquatic systems and soil, to acidification, to the contribution to the formation of tropospheric ozone, and therefore it constitutes an important precursor substance for the formation of summer smog (1–3). As in addition NO and NO_2 are toxic and hazardous compounds per se (2, and references therein), there is a logical need to prevent or at least reduce the emission of NO_x.

With the invention of the three-way catalyst there is a very powerful and in fact successful tool at hand for the reduction of NO_x produced by engines which work under stoichiometric air to fuel conditions. On the other hand the development of a novel system for catalytic exhaust-gas after-treatment capable of reducing NO_x under lean gas conditions still remains a cardinal problem for those involved in automotive pollution control. Especially under the pressure of ever more stringent NO_x emissions limits, in combination with the need for a reduction in fuel consumption and hence CO_2 emissions, researchers have been striving to find a solution to the NO_x emissions problems related to lean-burn engines (4). Legislative pressure to develop an operative exhaust-gas after-treatment system for lean-burn engines might be exemplified by the fact that some countries, such as Brazil and Taiwan, even ban the sale of new cars equipped with diesel engines entirely (5).

Selective catalytic reduction using hydrocarbons as reducing agents (HC–SCR) has long been discussed as a feasible solution to the problem of removing NO_x in excess oxygen (6–9, and references therein). Unfortunately no catalytic system could be developed which fulfills all the needs, such as high selective NO_x conversion to N_2, hydrothermal stability, low light-off temperature, and a broad temperature window. Platinum group metals seem to be a favorable choice as active catalysts in this reaction (4). Most studies on platinum group metals concerning the reduction of NO were performed using Pt, Pd, and Rh; Ir so far has received comparatively little attention and was usually only used in multicomponent systems (10, 11). The limited use of Ir (injection engines from Mitsubishi) can be traced to several factors, among which the scarcity of Ir, problems with Ir loss due to the formation of volatile iridium chlorides and oxychlorides, and Ir's underestimated catalytic potential may be the most crucial ones. Only recently Ir was found to exhibit high activity in the reduction of NO in excess oxygen (12–14), and especially unsupported Ir (Ir black) was shown to exhibit high yields of N_2 (15–17). Most of the studies concerning NO decomposition and reduction have dealt with supported catalysts but only a few studies on NO

[1] To whom correspondence should be addressed. Fax: +41 1 632 11 63. E-mail: baiker@tech.chem.ethz.ch.

0021-9517/02 $35.00

decomposition were performed using unsupported platinum group metals, such as Pt wire (18, 19), Pt and Rh wire (20, 21), and Pt foil (22). More recently van den Broek *et al.* (23) reported on the low-temperature oxidation of NH_3 to N_2 over Pt and Ir sponge and found Ir sponge to be highly selective to N_2 due to the high activity of Ir for NO dissociation. Acke and Skoglundh studied NO reduction using propene, propane, and NH_3 as reducing agents over Pt black (24, 25). Except for Ir sponge in NH_3 oxidation, as mentioned above (23), and our own studies on Ir black in the HC–SCR process (15–17), unsupported Ir seems not to have been studied before. The use of unsupported material has many advantages. It enables the detailed investigation of the intrinsic catalytic activity of the respective metal, and the influence of metal dispersion can be assessed without interference from the support. Furthermore the synergies between the active metal and the mechanical mixing components (Al_2O_3, SiO_2, H–ZSM-5) can be explored, and the comparison between supported and unsupported materials allows an estimation of the influence of metal carrier interaction on catalytic activity. Single reactions such as the reaction of NO, O_2, and the reducing agent with the metal can be studied without any disturbance from other components and reactions (such as adsorption and reaction of the reducing agent on the support, spillover of species from the metal to the support, etc.).

Here we investigate the behavior of Ir black under HC–SCR conditions and we focus on the relation between Ir crystallite size, $Ir : IrO_2$ ratio, and catalytic activity. Supported Ir–H–ZSM-5 systems, prepared according to a standard preparation procedure, are used to establish a relation between supported and unsupported Ir catalysts. Emphasis is put on the development of catalytic activity with time on-stream and the effects on crystallite size and the oxidation state of Ir. As larger crystallites (catalysts with lower metal dispersion) were found to exhibit significantly higher N_2 yields (12, 13, 15), we provide evidence that the increase in N_2 yield with increasing Ir crystallite size could be closely related to a change in the relative adsorption properties of O_2 and NO on Ir. Furthermore we studied the redox behavior of the systems Ir–O_2 and Ir–NO.

2. EXPERIMENTAL

2.1. Catalyst Preparation

Ir catalysts used in this study were prepared by wet impregnation of H–ZSM-5 (Si/Al = 34, 400 m^2/g, Chemie Uetikon). Two different aqueous solutions of Ir salts were used for impregnation: (A) $IrCl_3 \cdot 3H_2O$, and (B) $Ir(NH_3)_xCl_3 \cdot yH_2O$. Catalysts are accordingly denominated catalyst A and catalyst B, with actual metal loadings of 4.2, and 4.6 wt%, respectively. Iridium chloride (catalyst A) was obtain from Alfa Aesar and was used as the starting material for synthesis of the latter compound. Catalyst B is the product of refluxing an aqueous solution of $IrCl_3 \cdot 3H_2O$ with 25% NH_3 for several hours, subsequent removal of excess NH_3, and dilution with water.

After impregnation of the zeolite, the resulting catalysts were dried in air at 120°C for 12 h; catalysts A and B were either calcined in air at 500°C for 2 h (oxidized form) or reduced with 6% H_2 at 450°C for 6 h, heating, and cooling in N_2 (reduced form).

Ir black and IrO_2 were supplied by Alfa Aesar. These materials were either used as received or, to produce a certain crystallite size, presintered by heating in He to the corresponding set temperature with a heating rate of 10 K/min and then quenched to room temperature. Samples of Ir black were prereduced at 300°C with 6% H_2 prior to the catalytic tests. Energy-dispersive X-ray spectrometry, X-ray photoelectron spectroscopy, and X-ray fluorescence measurements did not reveal any significant impurities in the samples.

To distinguish supported catalysts from mechanical mixtures, for supported catalysts a dash was used to separate metal and support (Ir–H–ZSM-5) and for mixtures a slash was used (Ir/H–ZSM-5).

2.2. Mixing Material

The silica gel, which was used as mixing material, was prepared using the sol–gel method. The gel was prepared as xerogel using a solution of tetramethylorthosilicate (22.83 g) in *i*-propanol (105 ml) as starting material. A solution of H_2O (13.01 g) and HNO_3 (1.45 g) in *i*-propanol (40 ml) was added under vigorous stirring for hydrolysis. After 6 h of hydrolysis trihexylamine (6.06 g in 40 ml of *i*-propanol) was added and the gel was left to age for 6 days, dried in a vacuum oven at 50°C for another 5 days, and then calcined in air at 750°C for 3 h.

2.3. Catalytic Tests

For activity tests, 150 mg of the catalyst (particle fraction between 0.066 and 0.177 μm) was held between two quartz wool plugs in a quartz reactor (6 mm i.d.). The mechanical mixtures were prepared by dilution of Ir black with the mixing material, SiO_2. A reactor filling with a mixture of unsupported Ir black contained 7.5 mg of Ir black and silica to achieve a space velocity of approximately 80,000 h^{-1}. The feed gas contained 1800 ppm propene, 450 ppm CO, 300 ppm NO, 10% H_2O, 10.7% CO_2, 8% O_2, and N_2 as balance gas at a flow rate of 3 Nl/g/min. The term *in situ* conditioning represents the treatment of the catalysts for 4 h at 450°C with the above feed gas (heating in reaction atmosphere). Online analysis was performed using a Bruker IFS 66 Fourier transform IR spectrometer; details of the apparatus are described in Ref. (26). During steady-state experiments the temperature was gradually increased in steps of 50°C, starting at 160°C, with a holding time at each step of 1 h. For testing the influence of the time

onstream the catalysts were heated in N_2 to the set temperature, which was held for several hours after switching on the synthetic exhaust gas. After the experiments the catalysts were quenched in N_2 to room temperature.

The total consumption of NO is given as X_{NO} and NO conversion to N_2 (yield, Y_{N2}) was calculated according to the following equation (superscript 0 denotes inlet flows):

$$Y_{N2} = \left[\left(F^0_{NO} - (F_{NO} + F_{NO2} + 2 \cdot F_{N2O})\right)/F^0_{NO}\right] \cdot 100.$$

2.4. Characterization

X-ray diffraction (XRD). X-ray analysis was carried out on a Siemens D 5000 powder X-ray diffractometer using the CuK_α radiation in step mode between 20 and 80° 2Θ, with a step size of 0.01° and 4 s/step. The Ir crystallite size was estimated using XRD line broadening of the Ir(111) reflection and the Scherrer equation, taking 0.9 as a shape factor value.

Thermal Analysis (TA). Thermoanalytical experiments were carried out both isothermally and nonisothermally (heating rate 5 or 10 K/min) on a Netzsch STA 409 thermoanalyzer equipped with a gas injector (PulseTA box, Netzsch), which allows for the injection of a defined sample gas volume into the carrier gas stream (27). If not stated otherwise, the amount of injected gases (hydrogen, oxygen, nitric oxide) was 1.0 ml. Gases evolved during reaction and/or injected into the system were monitored online with a Balzers QMG 420 quadrupole mass spectrometer connected to the thermoanalyzer by a heated (ca. 200°C) capillary.

3. RESULTS

3.1. Change in Activity during Onstream Treatment of Ir–H–ZSM-5

It was found that the usually applied conditioning period of 4 h at 450°C (12) was not enough for Ir–H–ZSM-5 catalysts to reach their most active state. To study the influence of onstream conditioning on Ir–H–ZSM-5 in more detail, two Ir–H–ZSM-5 catalysts (catalysts A and B) with different crystallite sizes, prepared using two different Ir precursors, were treated onstream at 450°C for 16 h. This experiment was carried out with the reduced and oxidized forms of the respective catalysts. During this onstream treatment the development of NO conversion to N_2 (Y_{N2}) over time was monitored. The oxidized form of catalyst A was additionally kept onstream for 32 h to check whether steady-state could be reached by a further prolongation of the conditioning procedure. In contrast to the conditioning described in (12), in the experiments performed here the catalysts were heated slowly not in the reaction atmosphere but in N_2, to a final temperature of 450°C, and then the synthetic exhaust feed gas was switched on. This was to avoid any bias due to oxidation or reduction which could occur during heating in the synthetic exhaust gas and to be able to record the initial

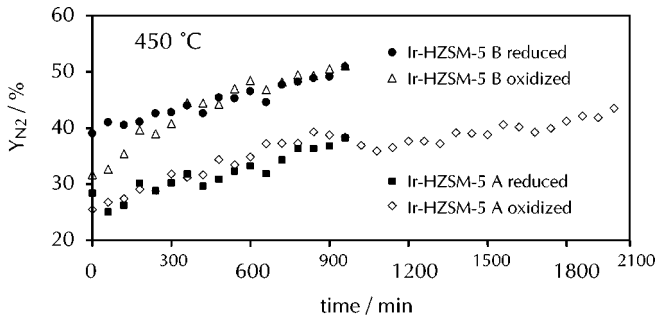

FIG. 1. Development of yield of N_2 of catalysts A and B (solid symbols reduced, open symbols oxidized) over time. The catalysts were kept at 450°C for 16 h under reaction conditions. Catalyst A was kept onstream for 32 h.

activity of a well-defined material at the specified temperature. Figure 1 shows the development of Y_{N2} over time. It can be seen that catalyst B starts at far higher Y_{N2} than does catalyst A and that the reduced form of catalyst B is initially superior to the oxidized form. The yield of N_2 increased with time onstream for both catalysts A and B, but a steady-state could not be reached after 16 h onstream. The oxidized form of catalyst A was treated 32 h onstream and the activity still improved slightly. The accompanying changes in Ir crystallite size and $Ir^0 : IrO_2$ are listed in Table 1. The reduced and the oxidized form of catalyst A behaved rather similarly, whereas with catalyst B the oxidized form was distinctly inferior, especially during the first 5 h of conditioning, to the reduced form. From Table 1 it emerges that catalyst A in all cases showed a lower Ir crystallite size and a lower content of Ir^0 compared to catalyst B. Irrespective of the initial oxidation state the treatment onstream led to the establishment of a certain $Ir : IrO_2$ ratio; this means

TABLE 1

Ir Crystallite Size and $Ir : IrO_2$ Ratio of Ir–H–ZSM-5 Catalysts A and B after Conditioning at 450°C[a]

Material	Time onstream (h)	Crystallite size before conditioning (nm)	Crystallite size after conditioning (nm)	$Ir : IrO_2$ after conditioning (mol%)
Ir–H–ZSM-5 A				
Reduced	16	4[b]	8[b]/8[c]	40 : 60
Oxidized	16	9[c]	4[b]/10[c]	34 : 66
Oxidized	32	9[c]	9[b]/9[c]	37 : 63
Ir–H–ZSM-5 B				
Reduced	16	14[b]	17[b]/9[c]	66 : 34
Oxidized	16	16[b]/14[c]	19[b]/7[c]	73 : 27

[a] The samples were heated in N_2 to 450°C, where the synthetic exhaust gas was switched on. The oxidized form of catalyst B (15 h at 500°C in air) initially contained 58% IrO_2. The $Ir : IrO_2$ ratio was determined by reduction of the catalyst samples after conditioning by pulses of hydrogen at 250°C.

[b] Ir crystallite size.

[c] IrO_2 crystallite size.

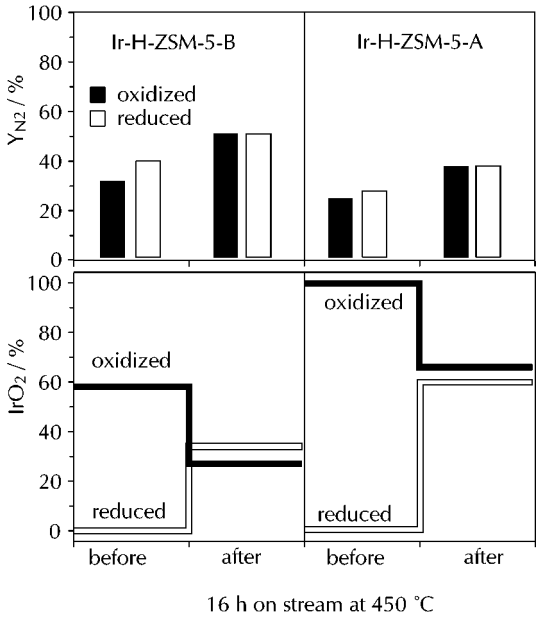

FIG. 2. Development of yield of N_2 and Ir : IrO_2 ratio of catalysts A and B (in reduced and oxidized forms) during conditioning at 450°C for 16 h under reaction conditions.

that under reaction conditions at 450°C, metallic Ir was oxidized and IrO_2 reduced. In all cases the treatment led to an increase in Ir crystallite size. This increase is somewhat smaller compared to the experiments in Ref. (12), where the catalysts were heated slowly in the reaction mixture to 450°C. Figure 2 summarizes the results for catalysts A and B concerning the development of the oxidation state and selective reduction of NO to N_2 over time. Irrespective of starting from the reduced or the oxidized form, the catalysts seem to approach a certain equilibrium in the Ir : IrO_2 ratio, which is approximately 1 : 2 for catalyst A and 2 : 1 for catalyst B. Y_{N2} before conditioning was usually somewhat lower for the oxidized catalysts but after conditioning the same values for Y_{N2} and similar values for the Ir : IrO_2 ratio were reached.

3.2. Change of Activity during Onstream Treatment of Ir Black Mixed with SiO_2

The influence of time onstream, initial crystallite size, and temperature on Y_{N2} and the Ir : IrO_2 ratio as well as crystallite growth for samples of Ir black were studied. The Ir black samples were mixed with silica to insure plug flow conditions. The samples were prereduced in 6% H_2 at 300°C for 30 min and then heated to the respective set temperatures of 350, 400, and 450°C; the final temperature was held for 11 h and the development of Y_{N2} was recorded. Figure 3 depicts the development of Y_{N2} vs time for samples with crystallite sizes of 3, 19, and 45 nm at 400 and 450°C. It emerges from Fig. 3 that the lower the crystallite size, the longer the time to reach a steady-state and the lower the values of Y_{N2}. An increase in temperature seemed to shorten the time to reach steady-state but for the samples with 3 nm even at 450°C steady-state was not achieved after 11 h. The results presented in Fig. 3 indicate that Y_{N2} of the sample with 45 nm did barely change over time (the slope of the interpolated line is near zero), whereas the 3-nm sample showed a large increase in Y_{N2} (as evidenced by the large positive slope of the interpolated line for 3 nm). The slope of the interpolated line for the sample with 19-nm size lies between the values of the two other samples. Table 2 describes the development of the crystallite size and the IrO_2 content of the investigated samples after activation at different temperatures. It clearly illustrates the fact that, as with the supported catalysts, the lager the Ir crystallite size, the smaller the ability to oxidize the catalyst during onstream treatment. Catalysts with an initial crystallite size of 19 nm or above did not or only very slightly sintered under reaction conditions. As expected, the sample with the lowest crystallite size exhibited the most pronounced changes. It showed the highest content of IrO_2 after all experiments and the crystallite size increased from 3 to 15 nm at 450°C. In contrast to the other samples this sample showed a decrease in oxide content with increasing reaction temperature. This is in line with the general dependence of oxidation on crystallite size: the higher the temperature, the more pronounced the Ir sintering and the lower the corresponding final oxide content. Figure 4 depicts the time necessary to reach 80% of the total change in Y_{N2}, which was achieved after 11 h at 400°C. The dependence that with larger crystallite size less time is necessary to reach steady-state holds true for 450°C as well, but the $t_{80\%}$ time was expectedly smaller than at 400°C (not shown).

Additionally, activity tests without SiO_2, using a catalyst bed of 100 mg of Ir black sintered to 27 nm, were performed according to the experiments described above; ordinary activity tests were as described in Refs. (12, 15). These experiments delivered results similar to those of experiments using mixtures of Ir and SiO_2, proving that the observed catalytic behavior is due to the Ir component alone and not influenced by some kind of interaction of Ir with the mixing material.

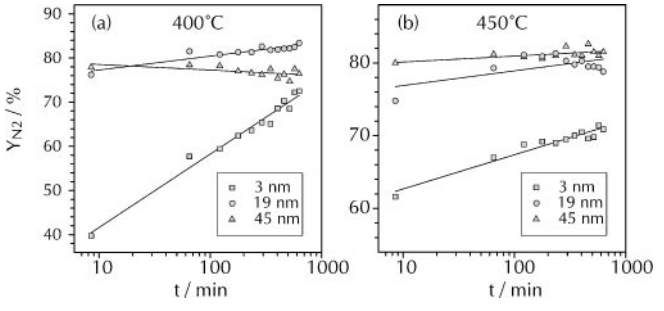

FIG. 3. Development of yield of N_2 for Ir black of different crystallite sizes (3, 19, and 45 nm) at 400 (a) and 450°C (b).

TABLE 2

Crystallite Size and IrO_2 Content of Samples of Ir Black with Different Initial Crystallite Sizes after 11 h at 350, 400, and 450°C

Initial crystallite size (nm)	Crystallite size after 350°C (nm)	IrO_2 content after 350°C (mol%)	Crystallite size after 400°C (nm)	IrO_2 content after 400°C (mol%)	Crystallite size after 450°C (nm)	IrO_2 content after 450°C (mol%)
3	9	13.1	12	12.4	15	11.8
5	10		13			
13	13		15			
19	19	7.5	19	8.7	21	10.8
27	27		27	5.4	27	8.2
45	45	0	45	0.9	45	2.0

Note. The IrO_2 content was determined by reduction of the catalyst samples after conditioning by pulses of hydrogen at 250°C.

3.3. Influence of Ir Crystallite Size on Reactions Occurring during HC–SCR

Steady-state activity tests up to 360°C, where usually a large difference in activity between the samples of different Ir crystallite size is found (NO_x light-off region), confirmed the differences in Ir : IrO_2 ratio during reaction for Ir black samples with different crystallite sizes. As in the usual activity tests (i.e., heating to a final temperature of 460°C), the samples were mixed with SiO_2 and heated in steps of 50°C from 160 to 360°C; at this temperature the reaction was stopped and the samples were quenched to room temperature in N_2. From Table 3 it can be deduced that even in the light-off region for NO_x reduction the usual tendencies are found: the larger the crystallite size, the lower the degree of Ir oxidation, and the less the tendency for further sintering. Figures 5A and 5B depict the conversion curves for the reductants, CO and propene. Note that with increasing crystallite size the light-off for the reductants is shifted to higher temperatures and that both reducing agents are completely consumed from 250°C on. It is interesting to note that the onset of propene consumption occurred at the same temperature where production of N_2O set in and the total consumption of the reductants occurred well below the light-off of NO_x reduction to N_2. This behavior was only found with prereduced samples; conditioned catalysts showed usually a simultaneous reductant and NO_x reduction light-off and exhibited higher yields of N_2. This coincidence of reductant light-off and NO_x reduction light-off has often been described before with platinum group metals in HC–SCR (for instance, Refs. 7, 28). In Figures 5C–F the situation for nitrogen-containing compounds is depicted. With increasing crystallite size the tendency to form N_2O at 210°C is reduced, NO_2 formation was totally suppressed on larger crystals, X_{NO} decreased with increasing crystallite size, and Y_{N2} at 360°C developed in the sequence $5 < 45 < 19$ nm, indicating that the increase in selectivity over larger Ir crystallites is partly offset by a reduction in X_{NO}, which is very likely due to the loss of specific surface area.

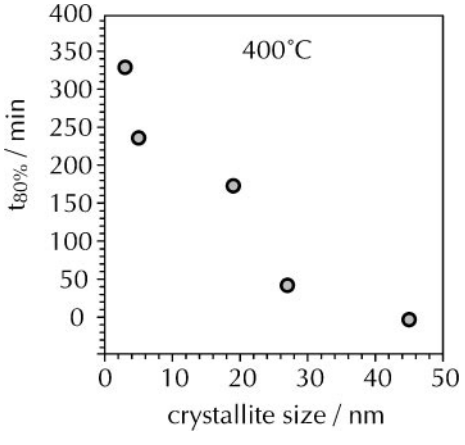

FIG. 4. Time required to reach 80% of the increase in yield ($t_{80\%}$) at 400°C vs crystallite size of Ir black.

3.4. Interaction of NO with Iridium

To better understand possible elementary steps which could occur in the HC–SCR process over Ir, the interactions of NO and Ir were studied more deeply. Though the Ir–NO system seems to be rather simple compared to a complete synthetic exhaust gas and Ir/SiO_2, as used above, it turned out that it exhibits rather complicated behavior. In the following, interactions between NO and crystalline IrO_2 are neglected because only weak adsorption of NO on crystalline IrO_2 was found and in Ref. (15) it was shown that IrO_2 was inactive for NO reduction. Furthermore, we found no interaction of NO with an XRD-amorphous IrO_2 precursor, which is formed during HC–SCR conditions (15) or by low-temperature adsorption of O_2 on Ir. Three

TABLE 3

Crystallite Size and IrO_2 Content after Activity Tests up to 360°C of Ir Black with Different Initial Crystallite Sizes

Initial crystallite size (nm)	Crystallite size after 350°C (nm)	IrO_2 content after 350°C (mol%)
5	9	9
19	19	5
45	45	0

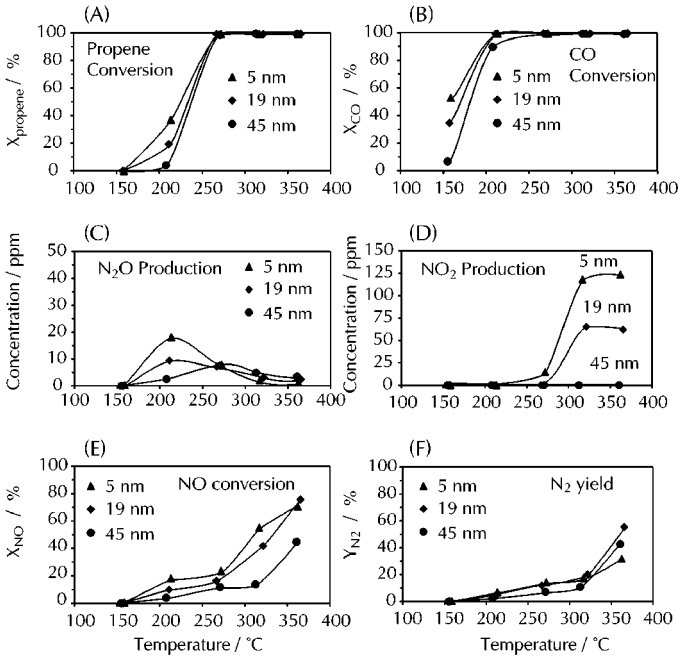

FIG. 5. Conversion of propene (A) and CO (B), production of N_2O (C) and NO_2 (D), total conversion of NO (E), and yield of N_2 (F). Experiments where carried out using Ir black with 5-, 19-, or 45-nm Ir crystallite size up to 360°C and using the complete synthetic exhaust gas. The temperature was increased stepwise up to 360°C from 160°C in steps of 50°C, with a holding time of 1 h per step.

different processes can occur during interaction of NO and metallic Ir:

1. decomposition of NO and formation of N_2:
$$Ir^0 + 2NO \rightarrow Ir\text{–}O_{ad} + N_2,$$
2. decomposition of NO and formation of N_2O:
$$Ir^0 + 4NO \rightarrow Ir\text{–}O_{ad} + 2N_2O,$$
3. adsorption of NO on the Ir surface:
$$Ir^0 + NO \rightarrow Ir\text{–}NO_{ad},$$

where Ir–O_{ad} and Ir–NO_{ad} correspond to adsorbed and/or reacted oxygen and NO, respectively. These processes differently depend on temperature, as emerges from the results summarized in Fig. 6. At room temperature a large fraction of NO chemisorbed on the Ir surface without reaction and only a small part of NO decomposed, leaving oxygen behind on the Ir surface. The contribution of processes 1 and 2 could be quantified by the determination of the amount of N_2 and N_2O formed during the pulse of NO and by quantifying the content of Ir–O_{ad} by reduction of the samples with H_2. The contribution of process 3 can be estimated from the quantification of the amount of N_2/N_2O formed due to a pulse of H_2 after the NO pulse (i.e., by the reduction of chemisorbed NO by H_2). This information together with the mass-gain and mass-loss of the sample due to NO and H_2 pulses, respectively, allows the estimation of the contribution of the various reactions to the overall process. As reactions 1–3 depend differently on temperature, with increasing temperature the fraction of NO decomposing over Ir increases, as depicted in Fig. 6C. At 500°C almost all NO in contact with Ir^0 was decomposed to N_2 and oxidized Ir^0 to IrO_2. Figure 6D illustrates that this increase in the contribution of the Ir oxidation to the overall mass-gain was mainly due to a decrease in the amount of chemisorbed NO and only to a relatively small increase in the oxidation of Ir. This implies reversible adsorption of NO on Ir and its strong temperature dependence. As adsorption of NO is a prerequisite for Ir oxidation by NO, the much smaller amount of adsorbed NO at higher temperature has the consequence that the amount of oxidized Ir due to a pulse of NO does not increase much with temperature. NO decomposition or NO dissociation over platinum group metals has often been interpreted as the main process leading to N_2 and to a poisoning of the active sites for NO decomposition with oxygen from NO (28, 29). Figure 6A shows the increase in N_2 and N_2O yield with temperature due to NO decomposition over Ir, and Fig. 6B illustrates the decrease in produced N_2/N_2O after reaction of the chemisorbed NO with a pulse of H_2, indicating the decrease in adsorbed NO. Due to three contributions to the intensity of the mass spectrometric signal of $m/e = 28$ (i.e., the presence of residual amounts of nitrogen in the TA-MS system, the fragmentation of N_2O, and the main signal originating from formed N_2), the concentration of N_2 and N_2O could be only roughly estimated. The maximum concentration of N_2O, detected at ca. 300°C, did not exceed 20–30% of the amount of N_2 formed. In the following, where significant contribution of

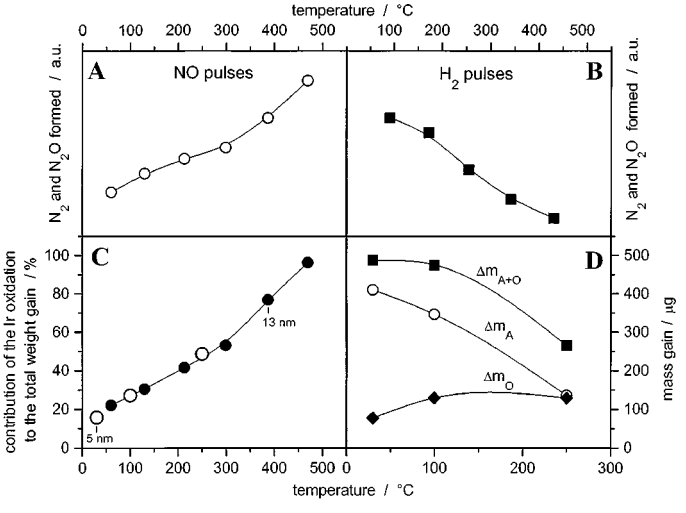

FIG. 6. Ir black with 13-nm crystallite size exposed to 1-ml pulses of NO at different temperatures (results for 5 nm are included as open circles): (A) amount of N_2 formed due to NO decomposition after a 1-ml pulse of NO; (B) evolution of N_2 due to pulses of H_2 after the NO pulse; (C) increase in NO decomposition compared to molecular adsorption with temperature. Ir black with 5 nm: (D) contribution of oxidation of Ir by NO (Δm_O) and adsorption of NO on Ir to the overall mass-gain (Δm_{A+O}).

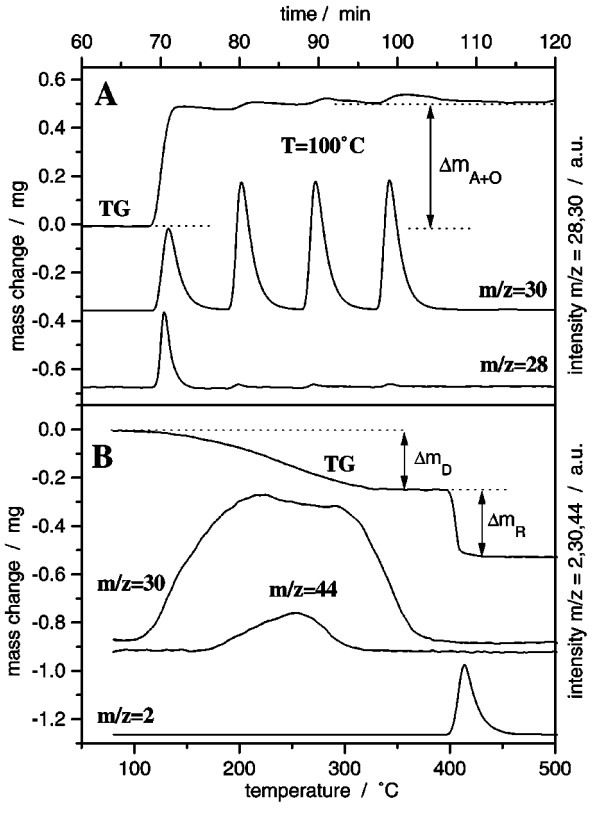

FIG. 7. (A) Pulses of 1 ml of NO over Ir black at 100°C illustrating NO decomposition (mass-gain accompanied by the evolution of N_2) during the first pulse and deactivation and saturation of the Ir surface by the following pulses. (B) Desorption of NO adsorbed at 100°C (heating rate 10 K/min) followed by reduction of the present oxygen by a pulse of 2 ml of H_2 at ca. 400°C.

N_2O to the N_2 signal could be excluded, $m/e = 28$ was considered representative for N_2.

Figure 7A depicts the adsorption of NO over Ir at 100°C. Results presented in Fig. 6 indicate that ca. 30% of the observed mass-gain was due to the deposition of oxygen on the Ir surface and 70% was due to the chemisorption of NO. It can be clearly seen that only the first pulse of NO (2 ml) led to significant formation of N_2. This indeed indicates the poisoning of active sites by oxygen produced from the decomposition of NO and the blocking of the rest of the reaction sites by NO adsorbed during the first pulse. The second pulse led to a very small further mass-uptake but the third pulse corroborated the fact that the surface had been saturated and all adsorption sites had already been occupied before. Further pulses of NO only led to a small temporary mass-gain, which is typical for weak adsorption and subsequent desorption. The temperature-programmed desorption of preadsorbed NO is depicted in Fig. 7B; this proves that NO, to a certain extent, is reversibly adsorbed on Ir. The mass-loss due to NO desorption (Δm_D in Fig. 7B) and integral intensities of $m/e = 30$ (NO), $m/e = 44$ (N_2O), and $m/e = 28$ (N_2 and N_2O fragmentation, not shown) allow the quantification of the processes occurring during desorption. About 66% of the NO chemisorbed at 100°C desorbed without reaction; the rest was decomposed during the desorption (ca. 26% NO reacted to N_2O and 8% to N_2), oxidizing the part of the Ir surface which was not oxidized during adsorption. The partial decomposition of NO on the Ir surface during desorption was reflected by the existence of a minimum centered at 250°C in the mass spectrometric signal of evolved NO ($m/e = 30$) accompanied by maxima in $m/e = 44$ and $m/e = 28$ signals (not shown). The amount of oxygen irreversibly adsorbed on the Ir surface during adsorption and desorption of NO was quantified using reduction by a pulse of H_2 at 400°C (mass-loss depicted as Δm_R in Fig. 7B). Desorption of NO was complete at ca. 380°C.

3.5. Influence of Iridium Crystallite Size on Reactions of Iridium with NO and O_2

The competition between NO and O_2 for adsorbing on and oxidizing Ir as well as their different affinities for oxidation of the reducing agent are key factors for explaining the selective reduction of NO over Ir. Triggered by the observation that large Ir crystallite size favors high yields of N_2 (Fig. 3), a closer look was taken at the changes in the reactions of NO and O_2 with Ir which are due to a variation in crystallite size.

The oxidation behavior of unsupported Ir was investigated at temperatures between ca. 200 and 450°C by injecting 1 ml of O_2. Figure 8 summarizes the oxidation of Ir black with different crystallite sizes. In Fig. 8A the pulse sequence at 350°C is depicted which was used to study the oxidation process. The pulse of 1 ml of O_2, which led to a certain mass-uptake of the catalyst sample, was followed by a pulse of H_2 removing the oxygen taken up before. This procedure was repeated several times to check reproducibility. The corresponding TG curves for samples with 5, 13, 27, and 45 nm Ir crystallite size show that the mass-uptake due to the O_2 pulse distinctly decreases with increasing crystallite size. Figure 8B shows the progress of oxidation of Ir samples having crystallite sizes of 13, 27, and 46 nm at different temperatures due to pulses of 1 ml of O_2. After each oxygen pulse, samples were reduced by hydrogen pulses. The results are in accordance with the tendencies observed in the catalytic tests where samples with the largest crystallite sizes were oxidized to the lowest degree, and the higher the temperature, the higher the oxide content. The sample with 45-nm crystallite size showed only a small but linear increase in mass-gain with temperature, whereas the sample with the smallest crystallite size exhibited a more pronounced increase in the slope of the interpolated oxidation rate at temperatures above 350°C. The inset in Fig. 8B depicts the relationship between the oxidation extent and crystallite size at 350°C. The sample with 13-nm size was oxidized to ca. 4%, whereas the sample with 45-nm size was only oxidized to less than 1%. With O_2 no reversible adsorption could be witnessed. Adsorbed O_2 formed an amorphous precursor of IrO_2 which crystallized between

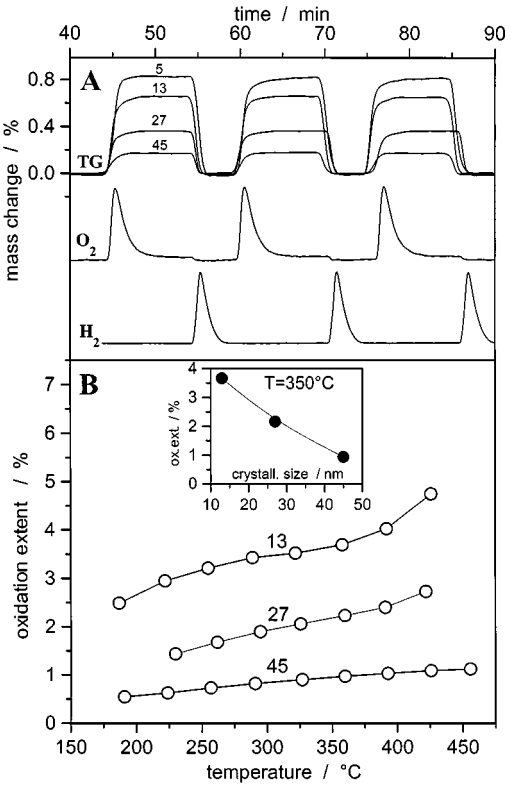

FIG. 8. (A) Pulse sequence used to investigate the mass changes of Ir black with crystallite sizes of 5, 13, 27, and 45 nm due to 1-ml pulses of O_2 and H_2. (B) Amount of irreversibly adsorbed oxygen on Ir black expressed as oxidation extent due to 1-ml pulses of O_2 as a function of temperature and Ir crystallite size (13, 27, and 45 nm). The inset represents the oxidation extent at 350°C as a function of crystallite size.

400 and 500°C to crystalline IrO_2, as detected by XRD. Only at temperatures above 800°C could decomposition of IrO_2 to Ir and O_2 be witnessed. The characterization of the phase formed due to adsorption of oxygen on Ir below 400°C is presently underway.

The differences described above in the interaction of NO and O_2 with Ir are further illustrated in Fig. 9. With increasing temperature, oxidation with O_2 led to a pronounced mass-gain, whereas with NO, processes 1–3 were contributing differently, depending on the temperature, to the overall process, leading to a net decrease in mass-uptake with temperature. Figure 9C depicts the interesting feature that after two 2-ml pulses of NO over Ir black, which is enough to saturate the Ir surface, as shown in Fig. 7A, a following pulse of 1 ml of O_2 led to a pronounced further mass-gain in the sample (see also Ref. 16). This could indicate that there are more adsorption sites available for O_2 than for NO. To check how this behavior depends on crystallite size, samples with various Ir crystallite sizes were subjected to the same series of pulses to compare their ability to react with Ir. To estimate the influence of temperature these experiments were performed over the range between 100 and 500°C. From Fig. 10A it emerges that with increasing

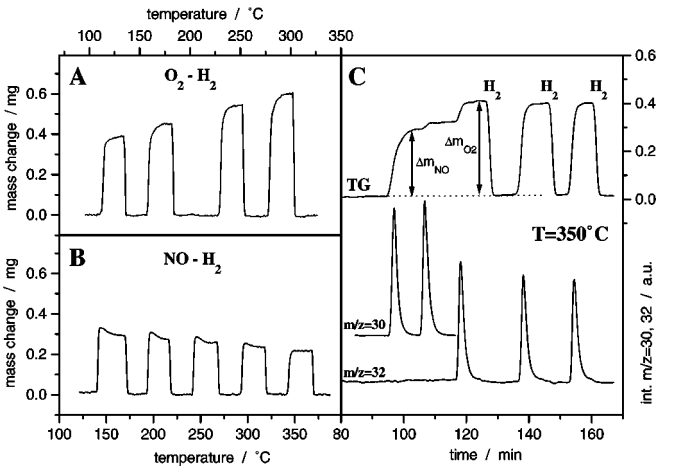

FIG. 9. (A) Mass-gain due to nonisothermal (heating rate 2 K/min) oxidation of Ir black by pulses of 1 ml of O_2 and subsequent reduction by H_2. (B) Mass-gain due to nonisothermal (2 K/min) adsorption/decomposition of NO over Ir and subsequent reduction by H_2. (C) Mass-gain due to adsorption/oxidation resulting from the injection of NO (2-ml pulse) and oxygen (1-ml pulse) over 27 nm of Ir at 350°C.

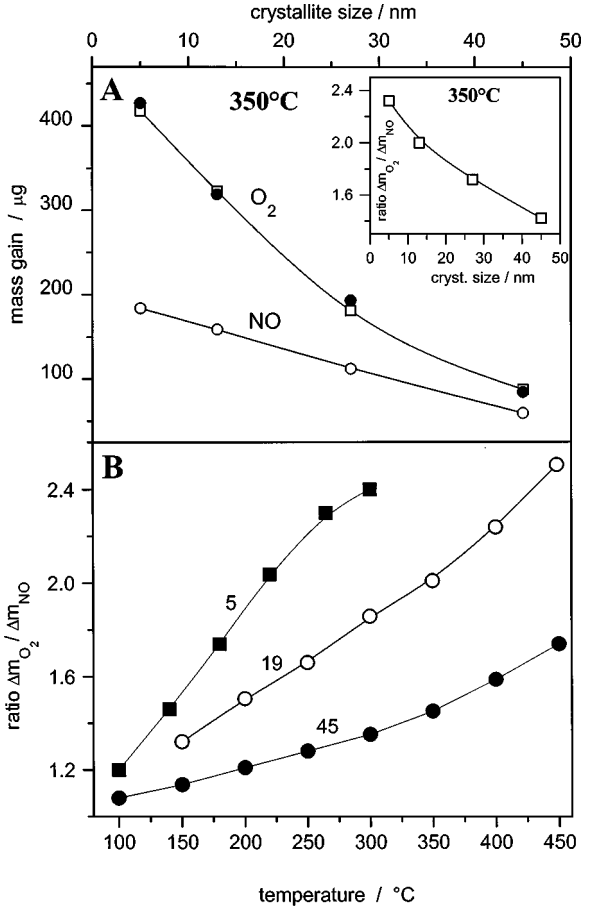

FIG. 10. (A) Influence of the crystallite size of Ir black on the ratio of the mass-gain due to the pulses of 2 ml of NO and 1 ml of O_2 at 350°C. (B) Dependence of the mass-gain due to deposition of oxygen on the Ir surface resulting from pulses of 2 ml of NO or 1 ml of O_2 on the crystallite size of Ir and on temperature.

crystallite size at 350°C the mass-gain due to oxidation by either reactant (NO or O_2) decreased but the decrease for oxidation by O_2 was far more pronounced. The inset in Fig. 10A presents the change in the ratio of the amount of oxygen adsorbed during O_2 pulses to the amount adsorbed after NO decomposition as a function of the crystallite size of Ir. In Fig. 10B this ratio is depicted as a function of temperature for samples with 5-, 19-, and 45-nm size. It is evident that this ratio is significantly smaller for larger crystals than for smaller ones. The slower increase in this ratio for the 5-nm sample at temperatures above 250°C is due to the increase in its crystallite size at higher temperatures. The larger the Ir crystallite size, the smaller the difference between the oxidation ability of both gases. All results presented in Fig. 10 indicate that the size of active adsorption centeres for NO is distinctly smaller than for O_2, but for larger Ir crystallite size a relative increase in NO adsorption centeres is found. This observation could explain the increased selectivity of the NO reduction process over Ir with increasing crystallite size.

4. DISCUSSION

For both supported and unsupported Ir catalysts, conditioning onstream proved to be beneficial, as reported previously in Ref. (12). This process leads to the establishment of a certain Ir : IrO_2 ratio dependent on Ir crystallite size, time onstream, and temperature. For catalysts with small initial crystallite size it causes significant agglomeration/sintering. Although the mechanism of this agglomeration process of the iridium component may be influenced by the presence of chlorine on the supported Ir–H–ZSM5 catylysts (volatalization/redeposition of formed oxychlorides), with unsupported Ir black sintering is the most likely process leading to crystal growth under the conditions used. Morphological changes accompanied by crystal growth have been followed using XRD and electron microscopy (15). With unsupported Ir black ca. 20 nm seems to be a stable Ir crystallite size under the conditions applied in these experiments. All samples with smaller crystallite sizes were readily sintered up to values near 20 nm, while crystallite size of samples above 20 nm was not influenced markedly by onstream treatment. As expected, on supported Ir–H–ZSM-5 conditioning is far less effective compared to that on Ir black. This is reflected by the fact that Y_{N2} of the supported catalysts never reached values comparable to those of Ir black (ca. 50% compared to ca. 80%) and did not lead to steady-state even after 32 h onstream at 450°C compared to less than 1 h for Ir with 45-nm size at the same temperature. With the unsupported catalysts only the samples of Ir black with a very small initial crystallite size (3 nm) were still far away from steady-state conditions after 11 h onstream.

With the Ir black sample of 3-nm Ir crystallite size, the superposition of the effects of crystallite growth and Ir oxidation can be observed. After keeping the samples 11 h onstream at 350, 400, and 450°C, the sample with 3-nm initial crystallite size had the highest content of IrO_2 compared to all other samples, but due to the growing crystallite size of this sample, the IrO_2 content after reaction decreased from the 350–450°C experiment. With the 19- and 45-nm-sized samples, the IrO_2 content increased with increasing temperature and no further crystallite size growth was observed.

The experiments depicted above confirm the strong influence of Ir crystallite size on the HC–SCR process. A dependence of $DeNO_x$-activity of Pt-based catalysts on particle size has been mentioned before, in Refs. (7, 28), which claim that catalysts with higher Pt dispersion exhibit lower activity compared to catalysts with lower dispersion. For Rh catalysts similar findings were published on the reduction of NO by CO (30–32), but it seems that for Ir catalysts in HC–SCR this effect of dispersion is most pronounced (12, 13, 15). It influences redox behavior and hence the activity and selectivity of the reactions involved. The observed tendencies are quite clear: increasing crystallite size decreases the degree of oxidation of the samples and the time to reach steady-state; it also increases Y_{N2} as well as selectivity to N_2 and strongly disfavors oxidation of NO to NO_2. It is interesting that catalysts with the lowest degree of oxidation are the most active and are even more active than is completely reduced, metallic Ir black. It seems that a certain degree of surface oxidation, with the bulk of the material remaining metallic Ir, enhances activity for NO reduction (see the results for unsupported Ir with 45-nm size). Assuming an NO decomposition mechanism as proposed for Pt by Burch and coworkers (28, 33) this may indicate that the reconstruction of the Ir surface by oxygen favors NO decomposition (34), but it may also indicate that hydrocarbon activation is facilitated (35). The described tendencies are confirmed by experiments using pure Ir black without mixing material. The results proved that the activity development we observed with supported Ir catalysts and in mixtures of Ir black with SiO_2 is mainly due to the intrinsic catalytic activity of the Ir component and not to an interaction between support or mixing material and Ir or Ir black, respectively.

Crystallite size was found to have an effect not only on oxidation behavior using O_2 as oxidation agent but also on the reaction of NO with Ir. These findings appear to be important for the explanation of the catalytic behavior of Ir. The results of the experiments of the oxidation of Ir by O_2 and NO differ considerably. Oxygen seems to be adsorbed irreversibly on the Ir surface whereas NO adsorption is partially reversible. The temperature dependence of irreversible oxygen adsorption on Ir is more pronounced for O_2 than for NO. The dependence of oxygen uptake on crystallite size also shows distinct differences for these reactants. The reactions of NO with Ir can be considered the superposition of three processes which differently depend on temperature: (i) (partially reversible) adsorption of NO on Ir, (ii) decomposition of NO and formation of Ir–O_{ad} leading

to N_2, and (iii) decomposition of NO and formation of Ir–O_{ad} leading to N_2O. It was found that with increasing temperature the percentage of NO which decomposes largely increases compared to the amount of NO adsorbed, leading to an increase in N_2 yield. This decomposition of NO over Ir results in self-poisoning, as has been confirmed before for Pt catalysts (28), and hence oxygen from NO is blocking active sites, leading to fast deactivation of the catalyst. This decomposition of NO was also described by Savkin and Kislyuk (34), who found NO decomposition to be more effective on Ir than on Pt. They also stated, similar to our findings, that with increasing temperature the adsorption rate of NO is rather low due to a very short lifetime of NO molecules on the Ir surface. This also explains why with increasing temperature the degree of oxidation of Ir by NO lags behind the degree of oxidation with O_2. Whereas O_2 is irreversibly adsorbed on Ir, not all NO molecules are capable of dissociating during the short lifetime on the Ir surface due to the fast desorption process. The temperature dependence of adsorption/desorption and decomposition of NO could also explain why the combustion of propene is strongly inhibited at lower temperatures (below 230°C) in the presence of NO, as described in Ref. (16). NO seems to be competing for the same surface sites as propene and at lower temperatures a major part of NO is chemisorbed on Ir and thereby blocks adsorption sites for propene. Only when enough NO is decomposed or desorbed again can propene oxidation proceed on the newly liberated adsorption sites. This also indicates that at lower temperatures no direct reaction between propene and adsorbed NO occurs.

The fact that after saturation of the catalyst with NO by pulsing several pulses of NO over Ir black a pulse of O_2 still leads to a further mass-gain (i.e., oxidation of the sample) is an indication that NO and O_2 can adsorb on the Ir surface at different sites. NO seems to only selectively adsorb and react on certain surface sites, whereas O_2 adsorption is rather indifferent to the nature of sites. With increasing crystallite size the ratio of NO adsorption sites to O_2 adsorption sites changes in favor of NO adsorption and/or reaction. The relative amount of sites on which only O_2 can react seems to decrease. This could be rationalized by the disappearance of edges and steps with increasing crystallite size on which O_2 could preferentially dissociate, or by an increase in the relative abundance of certain crystal faces which are active for NO adsorption/decomposition. These assumptions appear reasonable, as NO decomposition belongs to the group of structure-sensitive reactions (34) (i.e., the reaction rate is dependent on the crystal face). The above-described difference between O_2 and NO is a significant finding for the question of why with increasing crystallite size NO reduction is favored over NO oxidation in an oxygen-containing atmosphere. The decrease in oxygen concentration has two important consequences: it reduces the chance for NO to be oxidized to NO_2 and it diminishes unselective hydrocarbon consumption, affording increasing reductant efficiency. The catalytic tests confirm this behavior: for Ir with larger crystallite size we observe less production of NO_2 and higher yields of N_2.

5. CONCLUSIONS

Studies on the structure sensitivity of HC–SCR of NO over Ir catalysts have been combined with the investigation of the adsorption behavior of O_2 and NO. The efficiency of the NO reduction was found to be strongly influenced by Ir crystallite size. Ir crystallite size determines the time needed for the catalyst to reach steady-state under reaction conditions. The larger the crystallite size, the faster steady-state is achieved and the faster a certain Ir : IrO_2 ratio, together with high yields of N_2, is established. For supported catalysts, prepared according to standard catalyst preparation procedures, this process of reaching steady-state seems to be retarded by the metal-support interaction; unsupported Ir black reaches higher yields of N_2 in the reduction of NO by propene compared to supported catalysts. Ir black with a crystallite size below 20 nm sinters under HC–SCR conditions. NO adsorption on Ir^0 was found to be partially reversible, whereas O_2 adsorption is irreversible. Furthermore NO selectively adsorbs on certain surface sites, whereas O_2 adsorption seems to be indifferent to structural differences on the Ir surface. With increasing crystallite size the number of sites on which only O_2 can adsorb decreases and thus the ratio of the surface concentration of NO to O_2 changes in favor of NO. This leads to a reduced probability of NO oxidation and unselective hydrocarbon consumption. This seems to be a key factor responsible for the pronounced improvement in selective conversion of NO to N_2 with increasing Ir crystallite size.

ACKNOWLEDGMENT

We thank dmc^2 Degussa Metals Catalyst Cerdec AG for financial support of this research project.

REFERENCES

1. "Guidlines for Air Quality," available at http://www.who.int/ peh/.
2. Fritz, A., and Pitchon, V., *Appl. Catal. B* **13**, 1 (1997).
3. "Air Pollution in Europe," EEA, Environmental Monograph No. 4., (A. Jol and B. Kielland, Eds.), Office for Official Publications of the European Community, Luxenburg, 1977.
4. König, A., Herding, G., Hupfeld, B., Richter, T., and Weidmann, K., *Top. Catal.* **16/17**, 23 (2001).
5. Walsh, M. P., *SAE* P-990107 (1999).
6. Akama, H., and Matsushita, K., *Catal. Surv. Jpn.* **3**, 139 (1999).
7. Burch, R., and Millington, P. J., *Catal. Today* **26**, 185 (1995).
8. Farrauto, R. J., and Heck, R. M., *Catal. Today* **51**, 351 (1999).
9. Pârvulescu, V. I., Grange, P., and Delmon, B., *Catal. Today* **46**, 253 (1998).
10. Nakatsuji, T., Yasukawa, R., Tabata, K., Ueda, K., and Niwa, M., *Appl. Catal.* **21**, 121 (1999).
11. Takami, A., Takemoto, T., Iwakuni, H., Yamada, K., Shigetsu, M., and Komatsu, K., *Catal. Today* **35**, 75 (1997).

12. Wögerbauer, C., Maciejewski, M., Baiker, A., and Göbel, U., *Top. Catal.* **16/17**, 181 (2001).
13. Nakatsuji, T., *Appl. Catal.* **25**, 163 (2000).
14. Nawdali, M., Praliaud, H., and Primet, M., *Top. Catal.* **16/17**, 199 (2001).
15. Wögerbauer, C., Maciejewski, M., Baiker, A., and Göbel, U., *J. Catal.* **201**, 113 (2001).
16. Wögerbauer, C., Maciejewski, M., and Baiker, A., *Appl. Catal. B* **34**, 11 (2001).
17. Wögerbauer, C., Maciejewski, M., Schubert, M. M., and Baiker, A., *Catal. Lett.* **74**, 1 (2001).
18. Green, T. E., and Hinshelwood, C. N., *J. Chem. Soc.* **128**, 1709 (1926).
19. Pancharatnum, S., Lim, K. J., and Manson, D. M., *Chem. Eng. Sci.* **30**, 781 (1975).
20. Bachmann, P. W., and Taylor, G. B., *J. Phys. Chem.* **33**, 447 (1929).
21. Zawadski, J., and Perlinsky, G., *Compt. Rend.* **198**, 260 (1934).
22. Amirnazmi, A., and Boudart, M., *J. Catal.* **39**, 383 (1975).
23. van den Broek, A. C. M., van Grondelle, J., and van Santen, R. A., *J. Catal.* **185**, 297 (1999).
24. Acke, F., and Skoglundh, M., *Appl. Catal.* **22**, L1 (1999).
25. Acke, F., and Skoglundh, M., *Appl. Catal.* **20**, 133 (1999).
26. Radtke, F., Köppel, R., and Baiker, A., *Catal. Today* **26**, 159 (1995).
27. Maciejewski, M., Müller, C. A., Tschan, R., Emmerich, W. D., and Baiker, A., *Thermo. Chim. Acta* **295**, 167 (1997).
28. Burch, R., Millington, P. J., and Walker, A. P., *Appl. Catal. B* **4**, 65 (1994).
29. Burch, R., and Watling, T. C., *Catal. Lett.* **37**, 51 (1996).
30. Oh, S. H., and Eickel, C. C., *J. Catal.* **128**, 526 (1990).
31. Hecker, W. C., and Breneman, R. B., *in* "Proceedings, Catalysis and Automotive Pollution Control, Brussels" (A. Crucq and A. Frennet, Eds.), Vol. 30, p. 257. 1986.
32. Kaspar, J., de Leitenburg, C., Fornasiero, P., Trovarelli, A., and Graziani, M., *J. Catal.* **146**, 136 (1994).
33. Burch, R., and Sullivan, J. A., *J. Catal.* **182**, 489 (1999).
34. Savkin, V. V., and Kislyuk, M. U., *Kinet. Catal.* **37**, 555 (1996).
35. Obuchi, A., Ohi, A., Nakamura, M., Ogata, A., Mizuno, K., and Ohuchi, H., *Appl. Catal. B* **2**, 71 (1993).